

Source of Acquisition  
CASI Acquired**UNCLASSIFIED****NACA**TECHNICAL LIBRARY  
RESEARCH MANUFACTURING  
3651-5951 SEPULVEDA BLVD.  
INGLEWOOD,  
CALIFORNIA**RESEARCH MEMORANDUM**

for the

4-16-44

Air Materiel Command, Army Air Forces

PERFORMANCE OF COMPRESSOR OF XJ-41-V TURBOJET ENGINE

IV - PERFORMANCE ANALYSIS OVER RANGE OF COMPRESSOR

SPEEDS FROM 5000 TO 10,000 RPM

By John W. R. Creagh, and Ambrose Ginsburg

Flight Propulsion Research Laboratory  
Cleveland, Ohio~~CLASSIFIED DOCUMENT~~

This document contains classified information affecting the National Defense of the United States within the meaning of the Espionage Act (USC 50:31 and 32). Its transmission or the revelation of its contents in any manner to an unauthorized person is prohibited by law. Information so classified may be imparted only to persons in the military and naval Services of the United States, appropriate civilian officers and employees of the Federal Government who have a legitimate interest therein, and to United States citizens of known loyalty and discretion who of necessity must be informed thereof.

Restriction/  
Classification  
CancelledTECHNICAL  
EDITING  
WAIVEDClassification  
CHAN  
By authority of  
Change by  
BAC**NATIONAL ADVISORY COMMITTEE  
FOR AERONAUTICS**

WASHINGTON

JANUARY 22 1948

**UNCLASSIFIED**

## NATIONAL ADVISORY COMMITTEE FOR AERONAUTICS

RESEARCH MEMORANDUM

for the

Air Materiel Command, Army Air Forces

## PERFORMANCE OF COMPRESSOR OF XJ-41-V TURBOJET ENGINE

## IV - PERFORMANCE ANALYSIS OVER RANGE OF COMPRESSOR

SPEEDS FROM 5000 TO 10,000 RPM

By John W. R. Creagh, and Ambrose Ginsburg

## SUMMARY

An investigation of the XJ-41-V turbojet-engine compressor was conducted to determine the performance of the compressor and to obtain fundamental information on the aerodynamic problems associated with large centrifugal-type compressors.

The results of the research conducted on the original compressor indicated the compressor would not meet the desired engine-design air-flow requirements because of an air-flow restriction in the vaned collector. The compressor air-flow choking point occurred near the entrance to the vaned-collector passage and was instigated by a poor mass-flow distribution at the vane entrance and from relatively large negative angles of attack of the air stream along the entrance edges of the vanes at the outer passage wall and large positive angles of attack at the inner passage wall. As a result of the analysis, a design change of the vaned collector entrance is recommended for improving the maximum flow capacity of the compressor.

## INTRODUCTION

At the request of the Air Materiel Command, Army Air Forces, an investigation of the XJ-41-V turbojet-engine compressor is being conducted at the NACA Cleveland laboratory to determine the performance of the compressor over a range of compressor (equivalent impeller) speeds and weight flows and to obtain fundamental information on the aerodynamic problems associated with large centrifugal-type compressors.

A preliminary investigation of the compressor was made at the equivalent impeller speed of 8000 rpm (references 1 and 2). An investigation was then made to determine the characteristics of the compressor over the range of speeds from 5000 to 11,500 rpm (design speed), but a complete failure of the compressor (reference 3) prevented obtaining data above the equivalent speed of 10,000 rpm. Another compressor, in which a suggested extension of the vaneless diffuser was incorporated, was then obtained, and a preliminary report on the performance of this compressor at equivalent speeds of 5000, 7000, 8000, and 9000 rpm is made in reference 4.

The results of the research conducted on the original compressor are summarized herein. Over-all performance data are presented for equivalent impeller speeds of 5000, 7000, 8000, 9000, and 10,000 rpm. The performance of the impeller and the diffuser as separate components is analyzed, and the variations in the flow angle of the air entering the vaned collector and of the air entering the simulated burner annulus are discussed. Information on the cause of the air-flow restriction in the compressor is included together with analysis of the air flow through the compressor. The possible benefits resulting from modifying the collector vanes and thereby extending the vaneless diffuser are also discussed.

## INSTRUMENTATION AND PROCEDURE

### Instrumentation

The compressor, the installation, and the instrumentation are fully described in reference 1. Standard pressure and temperature stations in the inlet pipe (references 5 and 6) together with 10 total-pressure, 13 static-pressure, and 15 temperature stations located in the simulated burner annulus were used to determine the performance of the compressor. Fifty-four static-pressure taps were used to measure the static-pressure variation along the flow path through the compressor, to calculate the impeller adiabatic efficiency, and to calculate the diffuser static-pressure-rise efficiency. A motor-operated, remote-indicating survey probe of the Fechheimer type (reference 7) was mounted on the compressor front cover and was used to measure the angularity and the total pressure of the air stream entering a typical vaned collector passage. This probe was installed normal to the air-flow-passage walls and approximately 1 inch ahead of the center of the entrance to a vaned collector passage, the distance being measured along the mean-flow-path line. Angles were measured relative to a radial line extending from the impeller axis. The motor-operated, remote-indicating yaw probe mentioned in reference 1 was used to determine the angularity of the air stream entering the simulated burner annulus.

### Procedure

The compressor was run at compressor (equivalent impeller) speeds of 5000, 7000, 8000, 9000, and 10,000 rpm. All runs were made with ambient inlet-air temperature and an inlet stagnation pressure of approximately 14 inches of mercury absolute except for the low compressor pressure ratios in the flow-cut-off range, where higher inlet pressures were used. Inlet pressures of 14 inches of mercury absolute were used in order that the complete range of compressor speeds might be investigated at the same inlet-pressure conditions with a 6000-horsepower driving motor. Surveys of the air stream were made at the entrance to the simulated burner annulus at 7000, 8000, 9000, and 10,000 rpm and at the entrance to the vaneed collector at 5000, 7000, 8000, and 9000 rpm.

### RATING METHODS

The performance of the compressor was based on the measured total pressures and temperatures at the impeller inlet and at the exit of the simulated burner annulus. Separate determinations were made of impeller and diffuser performance. The impeller performance was determined for each speed at a point in the vaneless-diffuser passage 1/8 inch from the impeller-exit blade tip. The total pressure was determined from the computed dynamic pressure and the measured static pressure. The calculations were made on the assumption that there was no change in total temperature of the air from the impeller tip through the system to the measuring stations in the simulated burner annulus, that the friction loss between the impeller exit and the measuring point was negligible, and that the velocity was constant across the diffuser passage. The air velocity and the density were determined from the measured static pressure, the continuity of flow, and the foregoing assumptions.

The vaneless diffuser and the vaneed collector were rated together as a complete diffuser. The diffuser efficiencies were determined from the following form of Bernoulli's equation for a gas:

$$\left(\frac{p_t}{p_s}\right)_1 = \left[1 + \frac{\gamma - 1}{2} \left(\frac{V}{c}\right)_1^2\right]^{\frac{\gamma}{\gamma-1}} \quad (1)$$

$$\left(\frac{p_t}{p_s}\right)_2 = \left[1 + \frac{\gamma - 1}{2} \left(\frac{V}{c}\right)_2^2\right]^{\frac{\gamma}{\gamma-1}} \quad (2)$$

where

$p_t$  stagnation, or total, pressure, inches mercury absolute

$p_s$  static pressure, inches mercury absolute

$\gamma$  ratio of specific heats

$V$  velocity of gas, feet per second

$c$  velocity of sound in gas, feet per second

Subscripts 1 and 2 refer to stations at the impeller exit and burner annulus, respectively. Values of  $V$  and  $c$  were determined from the measured total temperatures and the calculated static temperatures both at the impeller exit and in the burner annulus. If equal values of  $p_{t,1}$  and  $p_{t,2}$  are assumed then the ratio of equation (1) to equation (2) gives

$$\frac{\left(\frac{p_t}{p_s}\right)_1}{\left(\frac{p_t}{p_s}\right)_2} = \frac{\left\{\left[1 + \frac{\gamma - 1}{2} \left(\frac{V}{c}\right)_1^2\right]\right\}^{\frac{\gamma}{\gamma-1}}}{\left\{\left[1 + \frac{\gamma - 1}{2} \left(\frac{V}{c}\right)_2^2\right]\right\}^{\frac{\gamma}{\gamma-1}}} = \frac{p_{s,2}}{p_{s,1}}$$

which is the ideal static-pressure ratio. If the observed static-pressure ratio between these same two points is denoted by  $P$  then, with pressure ratios of 1.0 or less of no interest, the following equation defines the efficiency of the diffuser as used herein:

$$\text{diffuser efficiency} = \frac{1 - P}{1 - \left\{\frac{\left[1 + \frac{\gamma - 1}{2} \left(\frac{V}{c}\right)_1^2\right]}{\left[1 + \frac{\gamma - 1}{2} \left(\frac{V}{c}\right)_2^2\right]}\right\}^{\frac{\gamma}{\gamma-1}}}$$

This method of rating diffusers is outlined in greater detail in reference 8.

## RESULTS AND DISCUSSION

Compressor performance. - The compressor performance characteristics over the range of compressor (equivalent impeller) speeds from 5000 to 10,000 rpm are shown in figure 1. A peak adiabatic efficiency  $\eta_{ad}$  of 0.79 was obtained at a corrected equivalent impeller speed of 9000 rpm, a corrected weight flow of 48 pounds per second and a pressure ratio of 2.57. The maximum pressure ratio was 3.17 and occurred at 10,000 rpm at a corrected weight flow of 49 pounds per second and with an adiabatic efficiency of approximately 0.77. As shown on figure 1, the maximum corrected weight flow at 10,000 rpm was 63 pounds per second.

The compressor weight-flow variation with speed for maximum flow and for selected compressor efficiencies is shown in figure 2. The curves represent peak adiabatic efficiency, constant adiabatic efficiencies of 0.75 and 0.70, and maximum corrected weight flow. The turbojet-engine weight-flow design point of 78 pounds per second at rated speed of 11,500 rpm is also shown. Extrapolation of the maximum-weight-flow line to rated speed indicates that the maximum weight flow obtainable at rated speed will probably be below the engine-design requirement. Inasmuch as the 0.75 and 0.70 efficiency lines, which approximate the engine operating range, lie below the maximum-flow curve, it is evident that the compressor air-flow capacity at rated speed will be well below the design value.

The results of the surveys across the passage at the entrance to the simulated burner annulus are shown in figure 3 for maximum and peak-efficiency air flow at equivalent impeller speeds of 7000, 8000, and 9000 rpm. Angle readings were taken at 1/2-inch radial increments across the passage. At a speed of 10,000 rpm, a point survey at the center of the passage is shown. As described in reference 1, the tangential angle is the angle between the impeller axis and the vector representing the resultant of the axial and circumferential components of velocity. Only tangential angles are presented because, as shown in reference 1 and subsequent investigations, the radial angle was comparatively small and could be considered insignificant.

The curves show that the maximum variation in tangential angle was approximately  $30^\circ$  and that the greatest tangential angles were obtained at the lowest speed. It is evident that considerably more rotational than axial velocity existed, especially near the outer wall, and that, as the air flow decreased from maximum flow to peak-efficiency flow, the angle variation across the passage was reduced.

Very little change in air-flow-angle characteristics with speed was obtained at impeller speeds above 7000 rpm for either of the two operating conditions shown.

Compressor-component performance. - The compressor, impeller, and diffuser efficiencies are shown in figure 4.

The impeller-efficiency curves have a generally flat characteristic over the weight-flow range with peak efficiency at or near maximum compressor weight flow. The maximum calculated efficiency, 0.93, occurred at an equivalent impeller speed of 5000 rpm. The drop in impeller efficiency with increasing speed was small, the peak efficiency at 10,000 rpm being 0.89. The comparatively small variation in the impeller-efficiency curves indicates that the compressor flow restriction, or choking point, does not occur in the impeller, because choking in the impeller would result in pressure losses and a sharp drop in the impeller efficiency at the maximum-flow points. The relative values of impeller efficiencies indicate that this component has exceptionally good performance characteristics.

The values of diffuser efficiencies are considerably lower than the impeller efficiencies, a maximum value of 0.74 being obtained at 9000 rpm. In addition, the diffuser curves are quite peaked and, as the peaks of the impeller and diffuser curves do not coincide because of imperfect matching of these components, the over-all performance of the compressor was adversely affected. Of more importance, however, is the rapidity with which the diffuser efficiency falls off at the higher air flows, which indicates that pressure losses accompanying choking occurred somewhere in the diffuser. This choking is the primary cause of the expected failure of the compressor to reach the design air-flow value, as indicated in figure 2.

The relative effect of each component on the compressor performance is shown in figure 5, where a comparison is made of the static-pressure rise in both the impeller and the diffuser. In order to compare the static-pressure rise on a nondimensional basis, increments in static pressure are divided by the available total-pressure rise between the impeller inlet and the impeller exit. This ratio is shown for all speeds investigated and for that part of the weight-flow range between maximum flow and approximately peak compressor efficiency. The curves show that for all speeds, the impeller is converting a much greater part of the available total-pressure increase to static pressure. Combining this fact with the indicated high impeller efficiencies (fig. 4) shows that the impeller is the most effective compressor component. For

example, in the 10,000-rpm curves of figure 4, where a change in weight flow from 60 to 50 pounds per second increased the diffuser efficiency from 0.59 to 0.71, the impeller efficiency decreased from 0.89 to 0.87; the compressor efficiency, however, increased only from 0.75 to 0.77.

Flow capacity and flow limitations. - Figure 4 indicated that the diffuser was the compressor component limiting the maximum weight flow. Reference 2 points out that the choking point for an equivalent impeller speed of 8000 rpm occurred at the entrance to the vaned collector. Data from the present investigation show that this condition is true for all speeds from 5000 to 10,000 rpm. Figure 6 shows the static-pressure rise along the compressor flow path for an equivalent impeller speed of 10,000 rpm for maximum flow and for peak compressor adiabatic efficiency. The static-pressure taps are numbered to correspond with figure 7 of reference 2 and represent an arithmetic average of the inner and outer wall taps along the flow path except for the impeller section, where pressures along only the front cover were measured. At maximum flow a critical pressure drop occurred near the first static-pressure tap within the vaned collector passage.

Calculated Mach numbers at the point within the vaned-collector passage corresponding to the point of minimum static pressure (station 18 of fig. 6) are presented in figure 7. These Mach numbers were calculated using the form of the Bernoulli equation given in equations (1) and (2). Here  $p_t$  is the arithmetic average of the measured total pressure at the entrance to the collector vane as determined by pressure surveys across the flow channel and  $p_s$  is the measured static pressure at station 18 in the vaned collector passage. For weight flows corresponding to the choking point, Mach numbers of 1.0 were obtained for all speeds except 5000 rpm, where a condition of choked flow was never reached. For points along the constant-maximum-flow line, Mach numbers greater than 1.0 were obtained. Inasmuch as maximum flow corresponds to a Mach number of 1.0 in the vaned collector, choking near the entrance of the vaned collector was evidently responsible for the flow limitation.

The choking may be attributed to flow separation at the vane entrance with the resulting decrease in effective area available to the flow inasmuch as the effective flow area must be less than the geometric passage area if choking is to occur at the maximum observed flow rates. The flow separation may occur in a plane parallel to the impeller axis and a radius (separation from either the outer or inner walls of the channel) or in a plane normal to the impeller axis

around the leading edges of the collector vanes. Figure 8 shows the air-stream Mach number and the angle of attack as determined from surveys across the channel at the entrance to the collector vanes. Angle of attack is considered negative when the vector of incoming velocity is directed from the high to low pressure sides of the vane, which is opposite to conventional airfoil designation. Curves are presented for surge, peak adiabatic efficiency, and maximum flow at an equivalent impeller speed of 8000 rpm. The curves for the three different flow conditions show that the peak angle of attack and the peak Mach number shift from the inner wall at maximum flow to approximately the center of the passage for peak adiabatic efficiency and surge. The Mach number at the vane entrance for maximum flow is of the order of 0.6, which is relatively low compared with the high Mach number values at the critical flow region in the vaned collector passage, and indicates that the air-flow restriction occurred in the short flow-path length between the vane entrance and station 18 (fig. 6). Because a  $-15^\circ$  angle of attack represents only rotational flow, the air-flow distribution at the vane entrance for the choking flow condition indicates a reversal of the through-flow velocity at the outer passage wall and a piling up of the air on the inner passage wall. In addition, the angle of attack at the inner passage wall is too great for a satisfactory entrance air-stream distribution over the vane. The flow separation and the resulting flow restriction in the vaned collector passage are therefore believed to result from a combined effect of poor distribution of mass flow at the vane entrance and of the presence of relatively large negative angles of attack at the outer passage wall and large positive angles of attack at the inner passage wall.

#### SUMMARY OF RESULTS

A performance investigation of the XJ-41-V turbojet-engine compressor over an equivalent impeller-speed range from 5000 to 10,000 rpm, gave the following results:

1. A peak compressor adiabatic efficiency of 0.79 occurred at a speed of 9000 rpm. The maximum compressor total-pressure ratio at 10,000 rpm was 3.17, and the maximum corrected weight flow at this speed was 63 pounds per second.
2. The analysis of the compressor-flow-capacity characteristics indicated that at rated engine speed of 11,500 rpm the compressor flow capacity would be below the engine design requirements.

3. Angular surveys of the air stream at the entrance to the simulated burner annulus showed that for all speeds considerably more rotational than axial velocity existed, especially at the outer wall of the annulus.

4. The impeller rated as a separate component had flat efficiency curves over the weight-flow range at all speeds. Peak efficiency at a speed of 5000 rpm was 0.93 and at 10,000 rpm was 0.89.

5. The diffuser rated as a separate component had efficiencies considerably lower than the impeller efficiencies, a maximum value of 0.74 being obtained at a speed of 9000 rpm. The curves were quite peaked and indicated that the impeller and the diffuser were improperly matched for maximum compressor performance.

6. The compressor air-flow choking point occurred near the entrance to the vaned-collector passage and was instigated by a poor mass-flow distribution at the vane entrance and from relatively large negative angles of attack of the air stream along the entrance edges of the vanes at the outer passage wall and large positive angles of attack at the inner passage wall.

#### RECOMMENDATIONS FOR IMPROVING COMPRESSOR PERFORMANCE

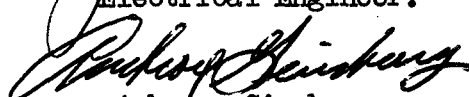
The XJ-41-V compressor probably will not meet the air-flow requirement of the turbojet engine and some change is necessary to increase its air-flow capacity. The analysis of the air-flow restriction indicated that the choking point occurred near the collector vane entrance and that the choking was instigated by separation in the vaned collector passage. The air-flow capacity may be increased by increasing the geometric flow area at the vaned collector entrance to give a greater available through-flow area and to provide for better mixing of the air stream. This recommended change can be obtained by cutting back the entrance edges of the collector vanes, which would result in an increased vaneless-diffuser radius.

Increasing the air-flow capacity in this manner would also tend to improve the efficiency of the compressor, for such an increase would shift the diffuser-performance curve to higher weight flows, where the peak efficiency of the impeller occurs. Fortunately the impeller performance is of such a high degree as not only

to permit the removal of flow-limiting restrictions in the diffuser but also to render highly probable the possibility of an increase in compressor efficiency at the same time.

Flight Propulsion Research Laboratory,  
National Advisory Committee for Aeronautics,  
Cleveland, Ohio.

  
John W. R. Creagh,  
Electrical Engineer.

  
Ambrose Ginsburg,  
Mechanical Engineer.

Approved:

Robert O. Bullock,  
Mechanical Engineer.

Oscar W. Schey,  
Mechanical Engineer.

rl

REFERENCES

1. Ginsburg, Ambrose, and Creagh, John W. R.: Performance of Compressor of XJ-41-V Turbojet Engine. I - Preliminary Investigation at Equivalent Compressor Speed of 8000 rpm. NACA RM No. E7A17a, Army Air Forces, 1947.
2. Dildine, Dean M., and Arthur, W. Lewis: Performance of Compressor of XJ-41-V Turbojet Engine. II - Static-Pressure Ratios and Limitation of Maximum Flow at Equivalent Compressor Speed of 8000 rpm. NACA RM No. E7E05, Army Air Forces, 1947.
3. Anon.: Aircraft Engine Division Engineering Report on Analysis of XJ-41-V Compressor Failure. N.A.C.A. Aircraft Engine Research Laboratory. Packard Motor Car Co., Aircraft Engine Div., June 5, 1947.

4. Creagh, John W. R., and Ginsburg, Ambrose: Performance of Compressor of XJ-41-V Turbojet Engine. III - Compressor Static-Pressure Rise at Equivalent Compressor Speeds of 5000, 7000, 8000, and 9000 rpm. NACA RM No. E7G03a, Army Air Forces, 1947.
5. Ellerbrock, Herman H., Jr., and Goldstein, Arthur W.: Principles and Methods of Rating and Testing Centrifugal Superchargers. NACA ARR, Feb. 1942.
6. NACA Subcommittee on Supercharger Compressors: Standard Procedures for Rating and Testing Centrifugal Compressors. NACA ARR No. E5F13, 1945.
7. Fechheimer, Carl J.: Measurement of Static Pressures. Mech. Eng., vol. 49, no. 8, Aug. 1927, pp. 871-873; discussion, pp. 873-874.
8. Bailey, Neil P.: The Thermodynamics of Air at High Velocities. Jour. Aero. Sci., vol. 11, no. 3, July 1944, pp. 227-238.

**Page intentionally left blank**

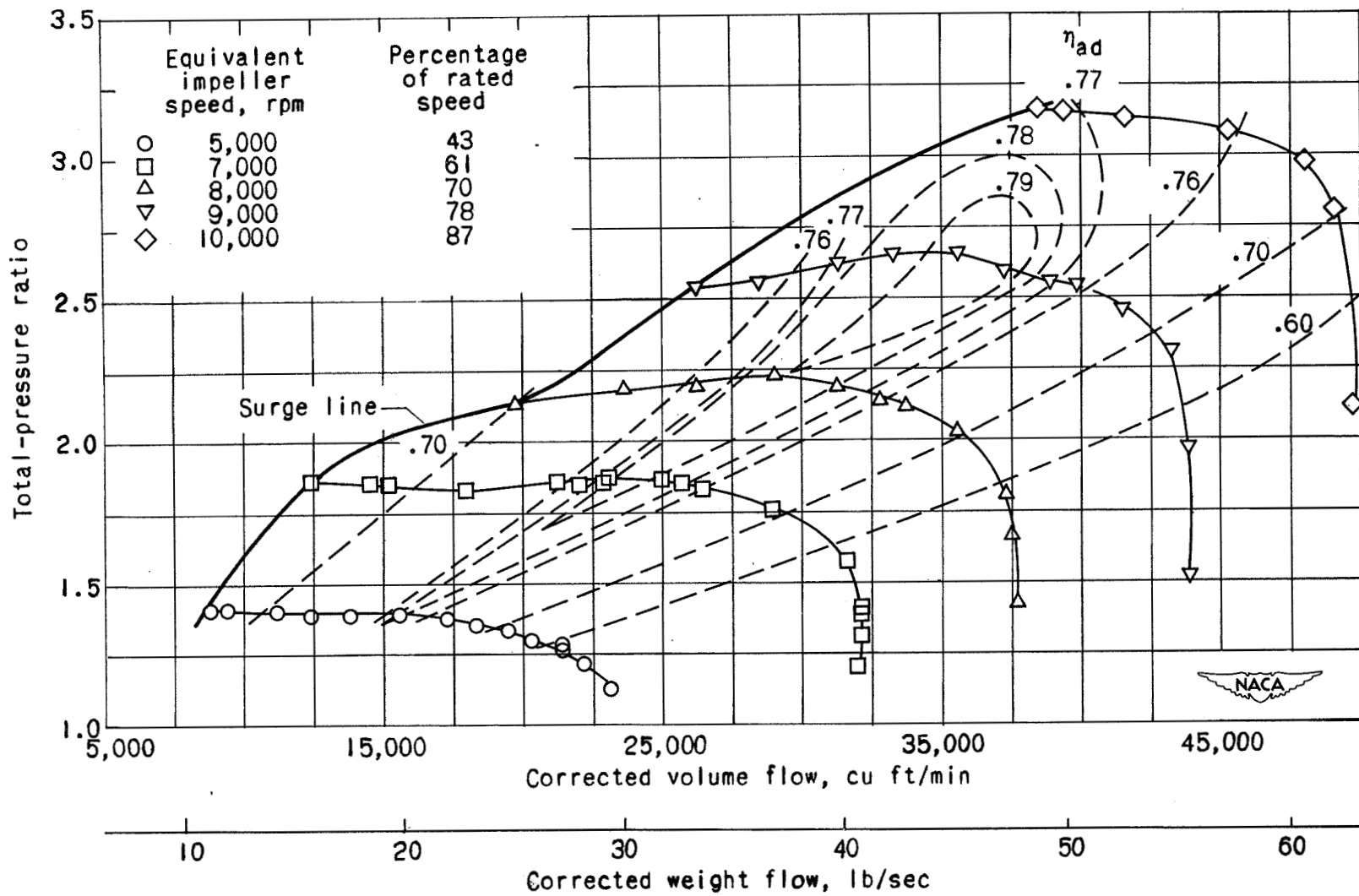


Figure 1. - Compressor performance.

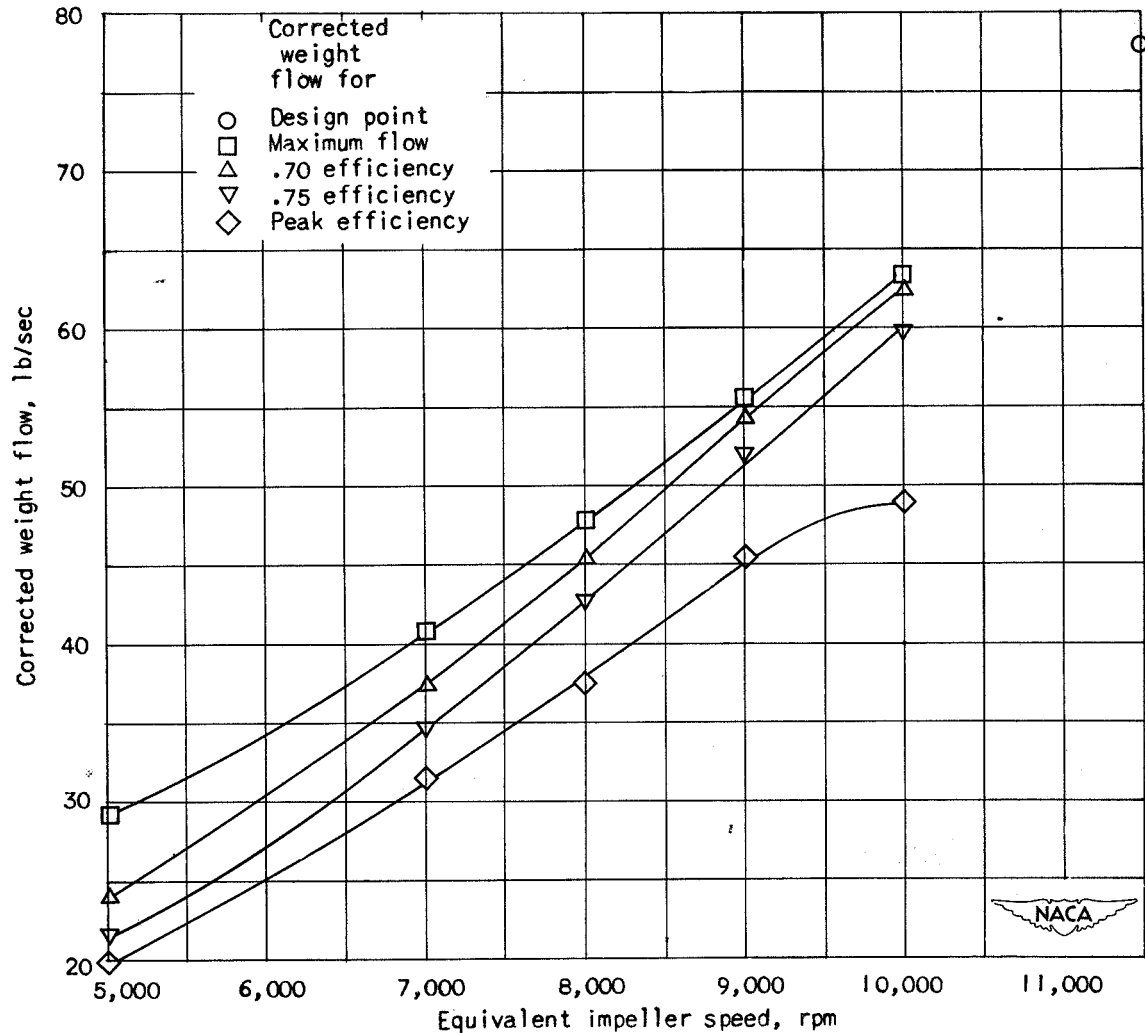


Figure 2. - Variation of weight flow with equivalent impeller speed for several compressor operating conditions.

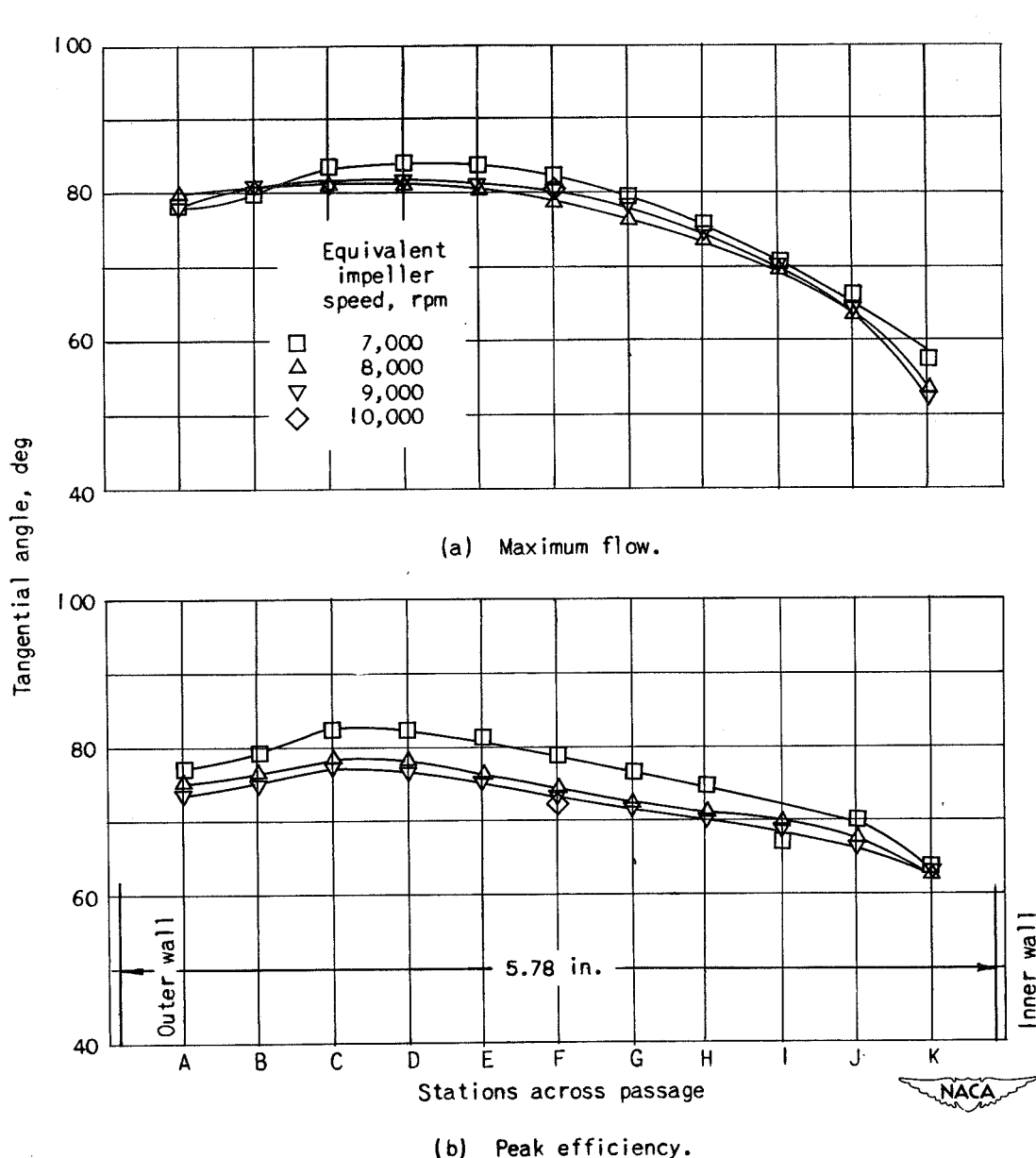


Figure 3. - Angular surveys at entrance to simulated burner annulus.

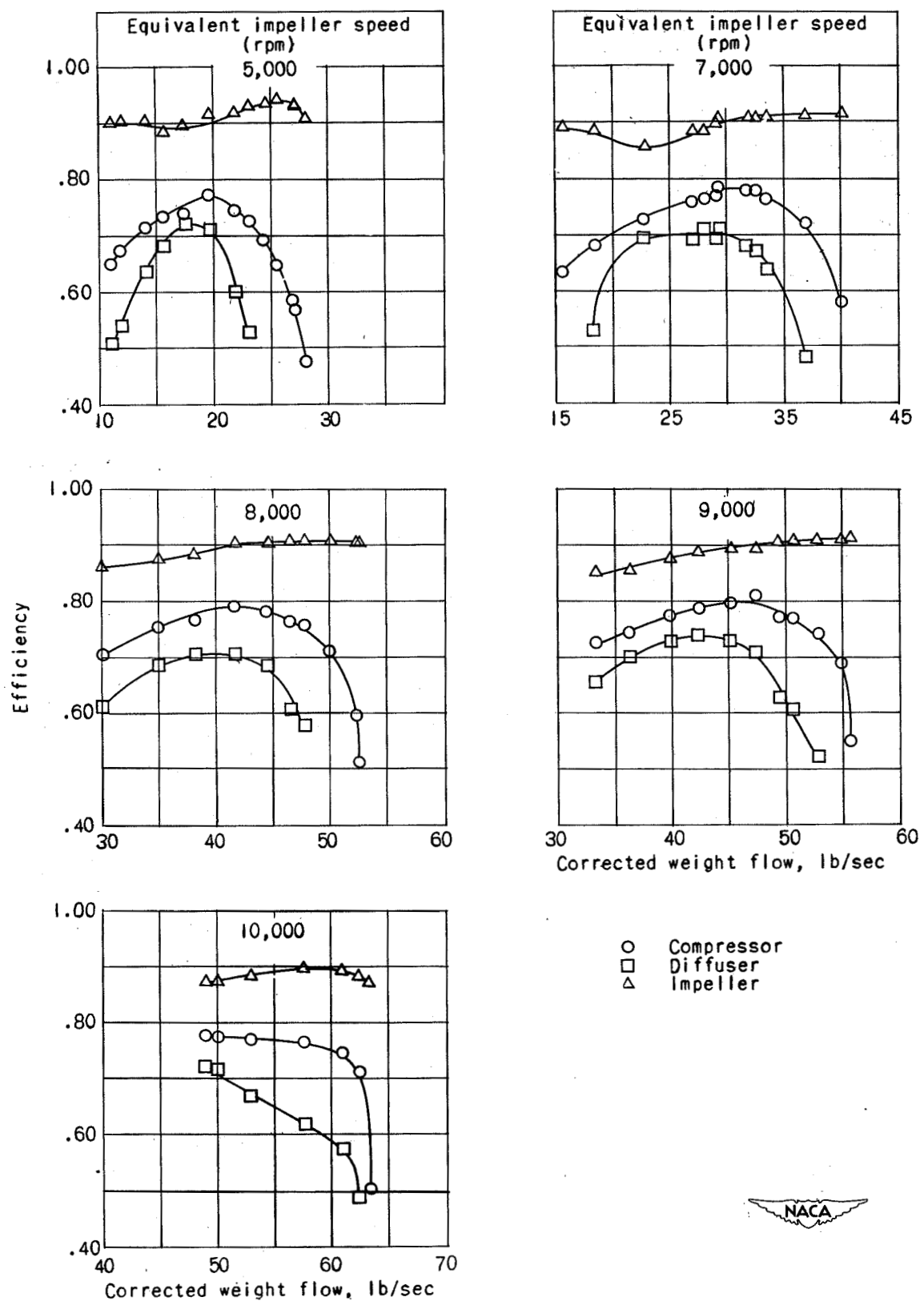


Figure 4. - Performance comparison of compressor, impeller, and diffuser for several impeller speeds.

NACA

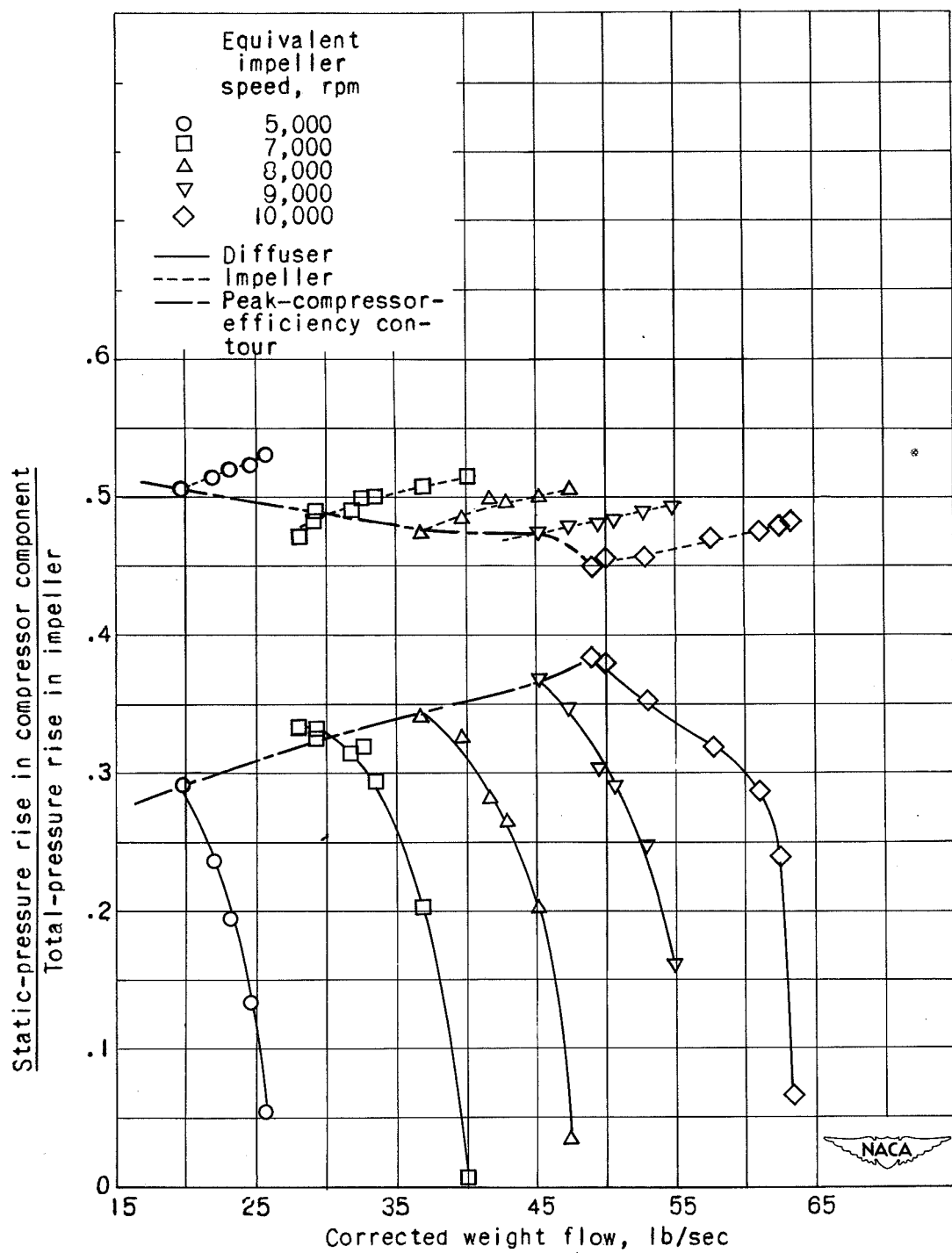


Figure 5. - Static-pressure-rise characteristics of impeller and diffuser.

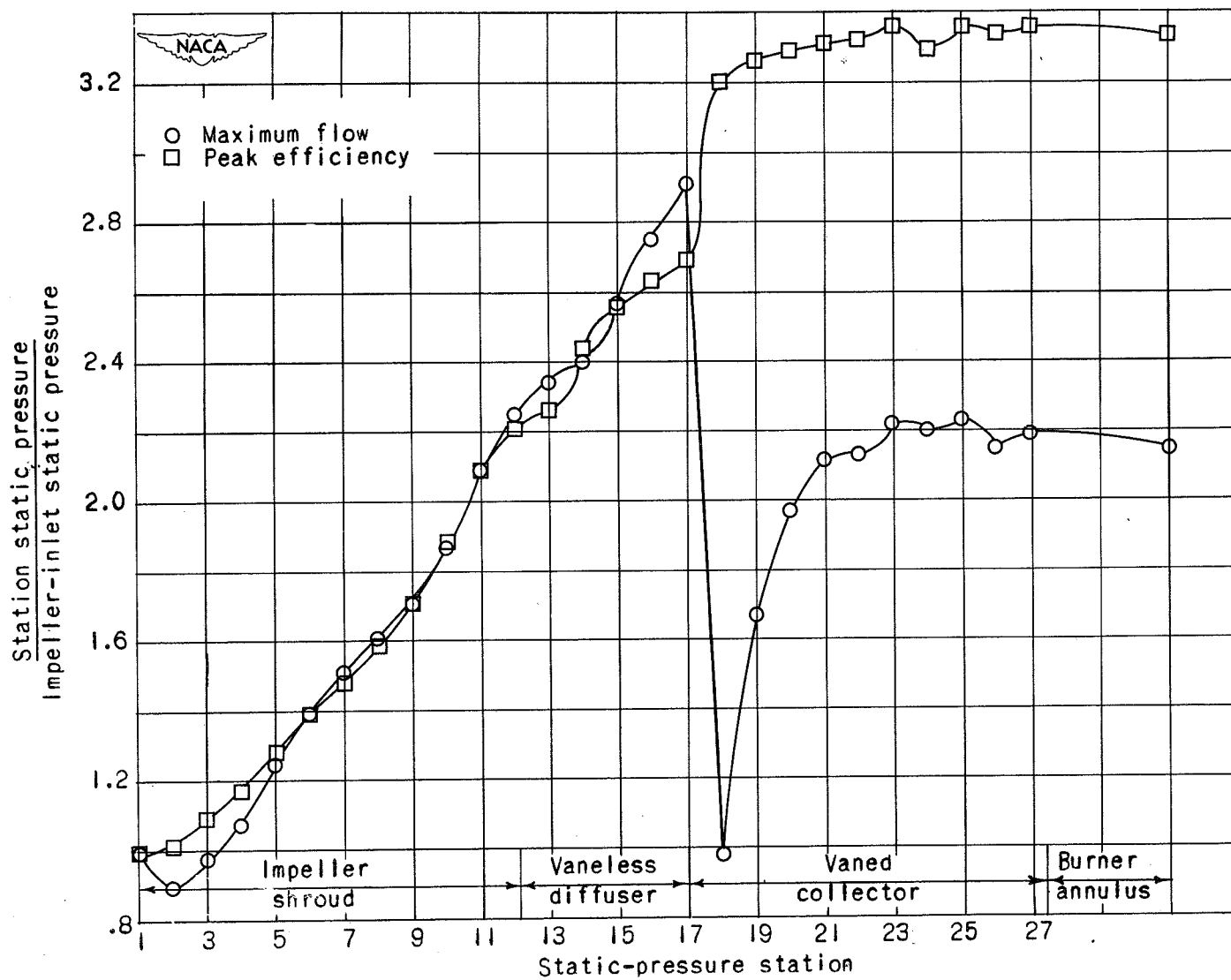


Figure 6. - Static-pressure variation through compressor at equivalent impeller speed of 10,000 rpm.

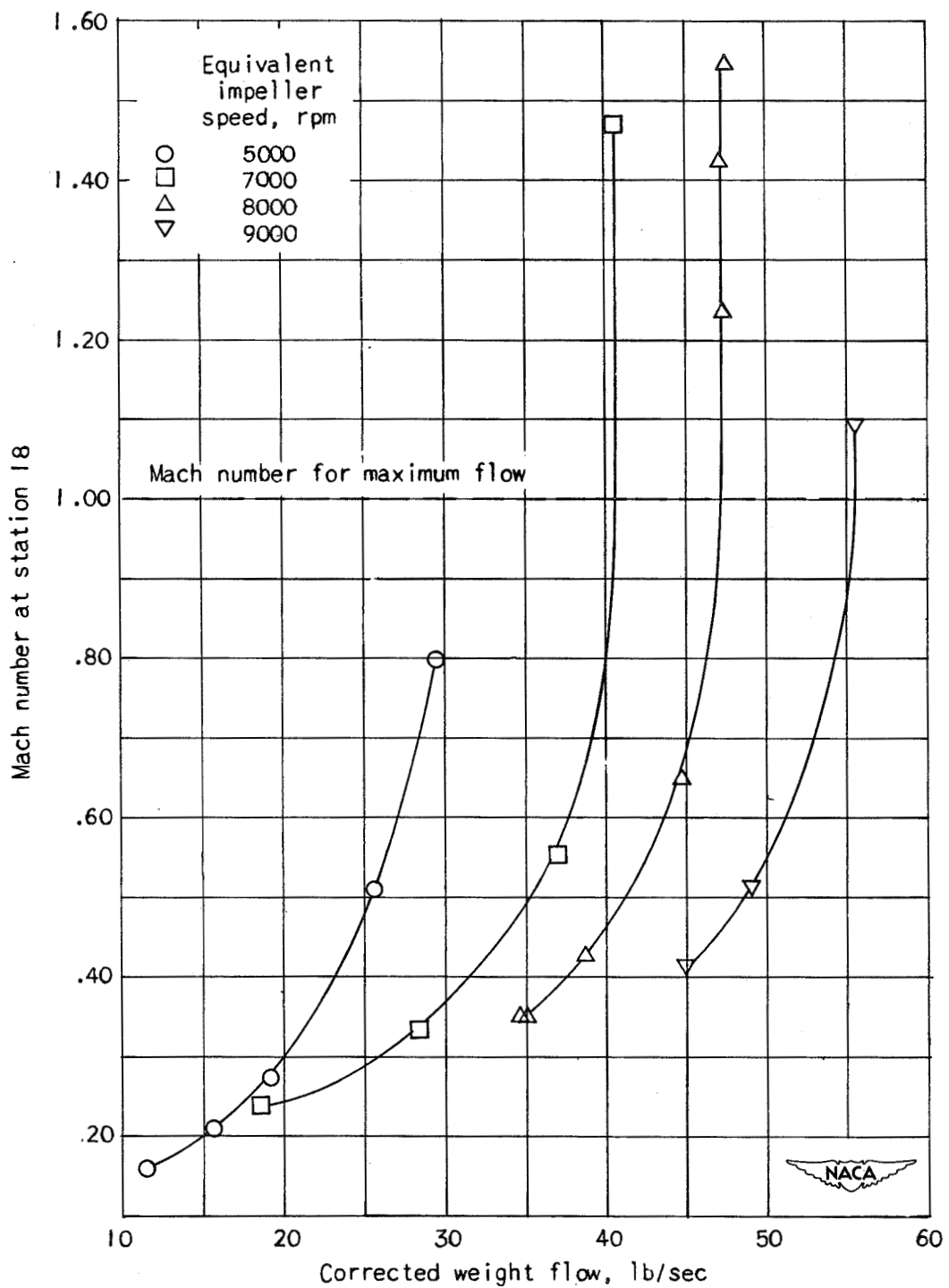
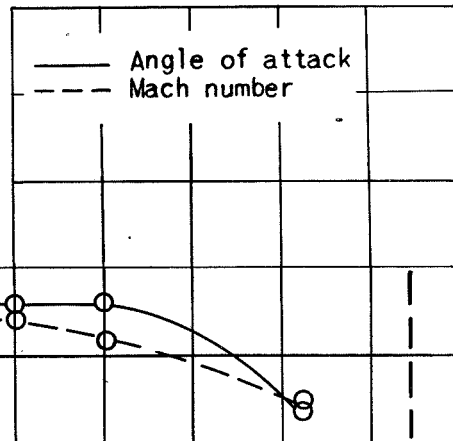
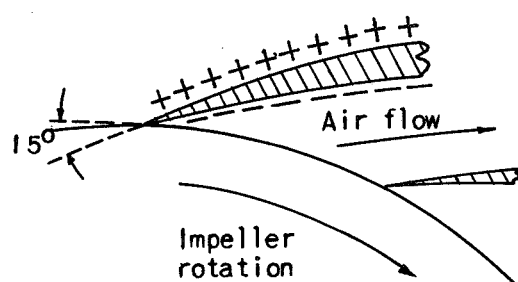
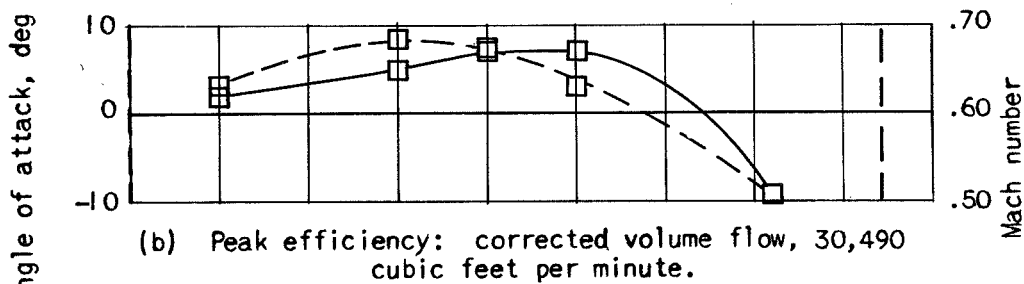


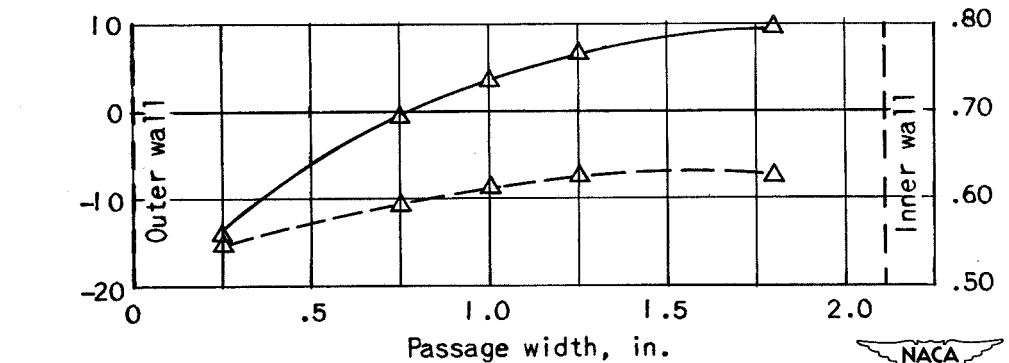
Figure 7. - Relation between Mach number near vaned-collector entrance and compressor weight flow.



(a) Surge: corrected volume flow, 23,500 cubic feet per minute.



(b) Peak efficiency: corrected volume flow, 30,490 cubic feet per minute.



(c) Maximum flow: corrected volume flow, 37,210 cubic feet per minute.

Figure 8. — Air-stream surveys at entrance to vane collector at equivalent impeller speed of 8000 rpm for various flow conditions.

NACA

**UNCLASSIFIED**

**UNCLASSIFIED**